Two-Photon Single Particle Tracking in 3-D

Peter T. C. So[*], Tim Ragan[%], Enrico Gratton[%], Jenny Carerro[%] and Edward Voss[%]

[*]Massachusetts Institute of Technology, Cambridge, MA 02139
[%]University of Illinois at Urbana-Champaign, Urbana, IL 61801

ABSTRACT

Transport processes are important in biology and medicine. Examples include virus docking and infection, endocytosis of extracellular protein and phagtocytosis of antigenic material. Trafficking driven by molecular motors inside a complex three dimensional environment is a shared common theme. The complex sequence of these events are difficult to resolve with conventional techniques where the action of many cells are asynchronously averaged. Single particle tracking (SPT) was developed by Ghosh and Webb to address this problem and has proven to be a powerful technique in understanding membrane-protein interaction. Since the traditional SPT method uses wide field illumination and area detectors, it is limited to the study of two-dimensional systems. In this presentation, we report the development of a 3-D single particle tracking technique using two-photon excitation. Using a real-time feedback system, we can dynamically position the sub-femtoliter two-photon excitation volume to follow the fluorescent particle under transport by maximizing the detected fluorescent intensity. Further, fluorescence spectroscopy can be performed in real time along the particle trajectory to monitor the underlying biochemical signals driving this transport process. The first application of this instrument will focus on the study of antigen endocytosis process of macrophages.

Keywords: SPT, two-photon, 3-D, microscopy, tracking, phagocytosis

2. INTRODUCTION

2.1, Significance of Single Particle Tracking in 3-D

An understanding of 3-D transport mechanisms is crucial in many areas of cellular biology including membrane receptor internalization and turnover[1-3], organelle transport during mitosis[4] phagocytosis of antigenic material[5-9], and nucleo-cytoplasmic trafficking of synthesized protein and nucleic acid[10]. In medicine, virus-membrane docking and the subsequent transfer of genetic material[11-14], endocytosis of protein toxin[15,16], and the invasion of intracellular bacterial pathogens[17-22] are major areas where an understanding of 3-D transport mechanisms would play a key role in disease prevention and treatment. Trafficking inside a complex three dimensional environment is a shared common theme. These trafficking processes are rarely passive or diffusion-controlled in cellular systems but are guided by active mechanisms including molecular motors and ion pumps[23,24].

Electron microscopy, pulse-chase biochemical assay and confocal 3-D microscopy are some of the methods used to delineate transport processes in cells. Electron microscopy has played a particularly important role in the understanding of receptor-mediated endocytosis. From the electron microscope images, localization of the receptor in clathrin coated pits and the subsequent localization and sorting in the intracellular vacuole has been visualized with nanometer resolution[2,25]. This further leads to molecular level structural understanding of the importance of clathrin in vesicle formation. Pulse-chase assays have allowed the internalization rate of membrane receptors and their recycle frequency to be measured[26,27]. Confocal microscopy sacrifices the ultra-resolution of the electron microscope but allows the study to be performed *in vivo*[28]. The success of these techniques is demonstrated by the fact that the outline of most of the transport pathways in cell biology has been established.

Despite our general understanding of these transport pathways, there are many important details of the transport mechanism missing. For example, it is not known whether ligand bound receptors are accumulated in the coated pit through passive diffusion or active transport; it is also unclear what are the steps or the speed for converting a coated pit into an intracellular

vacuole. The difficulties associated with understanding these fundamental processes are twofold. First, many of these motions are directed and under the active control of cellular mechanisms. These complex sequences of events are difficult to resolve when the action of many cells are asynchronously averaged. Second, many of these process are fast, on the order of milliseconds to seconds. Inherently static techniques such as electron microscopy cannot study these fast phenomena. There is a need for an alternative technology that can follow individual particles transported in three dimensions. SPT was first developed in the early 1980s to address this problem[29,30].

2.2 Background of single particle tracking (SPT) technology

The first SPT study followed the diffusion of membrane low density lipoprotein receptors in two dimensions[30]. This approach utilizes high sensitivity fluorescent imaging with a video rate intensified CCD camera and wide field illumination. Before the invention of this technique, one could only measure the average transport properties of these receptors as characterized by their membrane diffusion coefficient using techniques such as photobleaching recovery[31]. Using single particle tracking, non-equilibrium transport kinetic behavior has been observed; single receptors are shown to exhibit diffusive, restricted as well as directed motions[30,33,34]. The development of this technology has opened a new line of inquiry into the dynamics of membrane bound proteins. With few exceptions[32], most recent applications focus on measuring membrane protein interactions including studies of integrin-cytoskeletal interaction[35,36], diffusion of concanavalin A and Thy1 molecules in the plasma membrane[37,38], surface receptor movement during cell division[39], and lipid diffusion on a bilayer surface[40]. The scope of these studies is partially dictated by the two dimensional nature of the instrumentation and the plasma membrane provides a convenient and important two dimensional system.

As discussed previously, there are many important studies of biological processes which would benefit from particle tracking in three dimensions. The potential of using particle tracking in three dimensions was first realized by Kao and Verkman[41]. A cylindrical lens element was added to the excitation beam path to encoded a difference in the aberration pattern for a particle above and below the focal plane. Through a de-convolution routine during data analysis, they can recover the particle's trajectory in three dimensions. This technique has been successfully applied in the study of water permeability of Chinese hamster ovary cells. Although this technique constitutes a first step in developing a 3-D tracking technique, it has two major drawbacks that emphasize the need for an alternative technology. First, the axial tracking range of the instrument remains limited to 5 μm. At longer distances, tracking has to be interrupted and the stage repositioned. The axial positioning sensitivity is also not constant over the tracking range but diminishes at its limit. Second, the time resolution of this instrument is limited to video rate and cannot study many faster processes.

3. BASIC CONCEPTS UNDERLYING 3-D TWO-PHOTON SPT

The 3-D SPT instrument proposed is based on three basic concepts: two-photon excitation, active feed back control and interactive particle delivery

3.1. Two-photon excitation

This new 3-D particle strategy is based upon two-photon excitation. The application of two-photon excitation to microscopy was first introduced in 1990 by Denk[42]. Chromophores can be excited by the simultaneous absorption of two photons each having half the energy needed for the excitation transition[43,44]. Since the two-photon excitation probability is significantly less than the one-photon probability, appreciable two-photon excitation occurs only at a region of high temporal and spatial concentration of photons. The high spatial concentration of photons can be achieved by focusing laser light with a high numerical aperture objective to a diffraction limited spot. The high temporal concentration of photons is made possible by the availability of high peak power mode-locked (ML) lasers. For a mode-locked laser source with average power p_0, repetition rate f_p, pulse width τ_p, and wavelength λ, focused by an objective with numerical aperture A, the number of photon pairs absorbed per laser pulse and per chromophore, n_a, can be estimated as[42]:

$$n_a \approx \frac{p_0^2 \delta}{\tau_p f_p^2}\left(\frac{\pi A^2}{hc\lambda}\right) \qquad (1)$$

where c is the speed of light, h is Plank's constant and δ is the two-photon cross section, typically on the order of 10^{-50} to 10^{-49} cm^4 sec $photon^{-1}$ $molecule^{-1}$ [45,46].

In general, two-photon excitation allows 3-D biological structures to be imaged with resolution comparable to confocal microscopes but with a number of significant advantages: (1) Conventional confocal techniques obtain 3-D resolution by using a detection pinhole to reject out of focal plane fluorescence. In contrast, two-photon excitation achieves a similar effect by limiting the excitation region to a sub-micron volume at the focal point. This capability of limiting the region of excitation instead of the region of detection is critical. Photo-damage of the biological specimen is restricted to the focal point. Since out-of-plane chromophores are not excited, they are not subjected to photobleaching. Two-photon excitation ensures economical usage of fluorescent labels. (2) Two-photon excitation wavelengths are typically red-shifted to about twice the one-photon excitation wavelengths. This wide separation between the excitation and emission spectrum ensures that the excitation light and the Raman scattering can be rejected without filtering out any of the fluorescence photons. This improved sensitivity significantly improves the signal to background fluorescence ratio and is critical for tracking relatively dim objects. Further, this separation allows the spectroscopic properties across the whole emission spectrum to be monitored.

Depth discrimination is the most important feature of two-photon tracking applications. For one-photon excitation in a spatially uniform fluorescent sample, equal fluorescence intensities are contributed from each z-section above and below the focal plane assuming negligible excitation attenuation. This is a consequence of the conservation of energy[47]. On the other hand, in the two-photon case over 80% of the total fluorescence intensity comes from a 1 μm thick region about the focal point for objectives with numerical aperture of 1.25. Thus, 3-D images can be constructed as in confocal microscopy, but without confocal pinholes. This depth discrimination effect of two-photon excitation arises from the quadratic dependence of two-photon fluorescence intensity upon the excitation photon flux which decreases rapidly away from the focal plane. The spatial resolution of two-photon microscopy is comparable to one-photon methods. For excitation of the same chromophore, the two-photon resolution is roughly half the one-photon confocal resolution[48,49]. This reduction in spatial resolution is due to the larger diffraction limited spot of the longer wavelength two-photon excitation source (double the wavelength of the one-photon source). For a 1.25 N.A. objective using excitation wavelength of 960 nm, the typical point spread function has FWHM of 0.3 μm in the radial direction and 0.9 μm in the axial direction. Two-photon excitation does provide better suppression of higher order Airy rings. This localization of two-photon excitation can be best visualized in a simple bleaching experiment (Fig. 1).

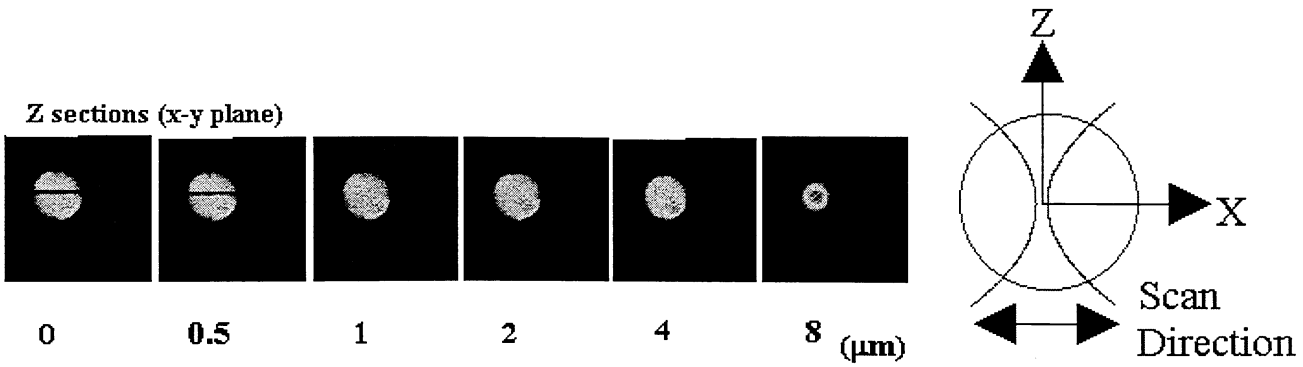

Fig. 1: A demonstration of the two-photon excitation localization effect. (a) The two-photon excitation volume was focused in the center of a 15 μm fluorescent latex sphere. The excitation volume was scanned repeatedly along the x-axis until photobleaching occurred. Afterwards, a 3-D image stack of the latex sphere was acquired. (b) The x-y planes of the sphere at increasing distance from the center are presented. No photobleaching is observed beyond 1 μm.

3.2. Active feedback control

Efficient two-photon excitation can only be achieved by focusing excitation to a diffraction limited spot. Two-photon imaging is inherently a sequential technique and is much slower than CCD imaging which is a parallel acquisition method. Therefore, the time required to gather a 3-D image stack is long. This is the same difficulty encountered in studies using

confocal microscopy. To circumvent this problem, we realize that it is unnecessary to image a whole cell to follow the path of a single particle. We only have to take a snapshot of the particle and its immediate surroundings. If we know the origin of this snapshot and if we can determine the centroid of the particle, we can relocate the origin of the next snapshot to center the particle in the next image. This active feedback control reduces the size of the scan volume and the time required to scan this volume. The ultimate time resolution of this tracking system will depend on the electronic and the mechanical elements of this feedback loop which will be discussed in the following section. As a side note, this active feedback tracking system can also work with confocal detection but many added advantages of two-photon excitation would be lost.

3.3. Interactive particle delivery

The active feedback tracking system can greatly increase the time resolution of this system but has one major limitation. In the presence of many small diffusing particles, the possibility of multiple particles entering into the excitation volume becomes appreciable. A smart feedback algorithm in the tracking system is critical and will help to alleviate this problem. Nevertheless, it is virtually impossible to guarantee against confusion when there is a high particle density. When the particles are identical, the only solution is to reduce the particle density such that the probability of having more than one particle in the volume of interest becomes negligible.

This low particle density criterion presents a problem. One example is the study of macrophage capture of antigens and there subsequent endocytosis. At very low antigen concentration, there is a very low probability that the antigen being tracked will interact with a macrophage cell. A solution to this problem is to actively deliver the particles to the vicinity of the area under study, in this case, the cellular membrane surface. Therefore, the third crucial element of this instrument is an active particle delivery mechanism. Two methods will be considered. The most straightforward technique of using micro-pipettes for delivery has the advantage that particles as small as single proteins can be manipulated. A second, more elegant, technique which works with larger particles (0.5 to 10 microns) such as bacteria and viruses is light gradient trapping[50,51]. In 1979, Ashkin discovered that due to the index of refraction difference between particles and the aqueous medium, a photon's path through a particle is deflected. This causes a transfer of photon momentum to the particle and generates a net force keeping the particle at the focal point.

4. SPECTROSCOPY AND SINGLE PARTICLE TRACKING

SPT is a unique technique which allows the itinerary of a transported particle to be precisely determined. However, one has to realize that the driving force behind the complicated transport process itself is biochemical in nature and the goal of transporting the particle is to position it at the proper cellular location to fulfill a certain biochemical function. The ability to assess the biochemical micro-environment around the transported particle is therefore essential. This aspect of the transport process has been overlooked in the traditional SPT experiments. SPT with two-photon excitation is an ideal opportunity to incorporate powerful fluorescence spectroscopic techniques.

Wavelength resolved spectroscopy has been used extensively in biological microscopy in three areas. First, the development of a large library of organelle and protein specific probes has allowed cellular components to be labeled and distinguished[52]. Using the multiple color labeling method, the cellular structures in the vicinity of the transported particle can be identified. Further, two-photon excitation has the unique property that the majority of known chromophores have appreciable two-photon cross-sections when excited in the 700-800 nm range[53]. Therefore, it is possible to simultaneously label, excite and image UV, blue, green and red chromophores bound to different structures. Second, fluorescent probes with fluorescent spectra sensitive to their biochemical environment has been developed. Cell permeant fluorescent probes designed to measure Ca^{2+}, K^{+}, pH, and membrane fluidity are readily available[52,54]. Using ratiometric imaging with these probes, the biochemical environment around the transported particle can be quantitatively monitored[55]. Third, sub-nanometer distance scales can be assessed with ordinary light microscopy by using fluorescence resonance energy transfer techniques[56].

Steady state polarization measures the time averaged orientation of the chromophore. In microscopy, the relative orientation of the particle in relation to known cellular structures, such as the plasma membrane, can be measured[57] providing structural information on the assembly of cellular components. The rotational diffusion coefficient of a particle can also be measured by polarization which provides valuable quantitative information on the cytoplasmic viscosity[58].

Lifetime resolved spectroscopy technique is relatively new in microscopy but its application has opened up many exciting new opportunities[59-63]. First, time-resolved imaging is a powerful contrast enhancing mechanism complementing wavelength resolved method. By labeling different organelles with dyes that have similar absorption spectra but different fluorescence lifetimes, these dyes can be excited and imaged with a single exposure and the organelles can be distinguished by their unique lifetime values. Under some circumstances time-resolved imaging is simpler and more efficient than the traditional multiple-color labeling method. Second, lifetime measurement is also a powerful method to complement spectral resolved method for quantitative measurement of cellular biochemical microenviroment. The excited state lifetime is an intrinsic property of a fluorescence probe, and is independent of the probe concentration. The lifetime is sensitive to the probe's micro-environment, and the lifetime may change with the presence of certain chemical species. Although ratiometric spectral imaging is a powerful method, there exists a large variety of biologically important chemical species for which there are no ratiometric probes available for quantitative measurement but can be measured using lifetime methods. For example, the all ratiometric calcium probes has their absorption maxima in the highly photodamaging UV region but efficient lifetime sensitive calcium probes are readily available in the longer wavelength region[64,65]. The concentration of other important metabolites such as O_2 can only be quantitatively measured by observing fluorescent quenching using lifetime method.

5. DESIGN OF A TWO-PHOTON SINGLE PARTICLE TRACKING MICRCOPE

The purpose of this section is to present a first generation two-photon single particle tracking system where the spectroscopic tools will be incorporated. This prototype instrument has been characterized by studying the diffusion of fluorescent latex spheres in solution.

5.1. Design of first generation prototype instrument

This prototype instrument was built in the LFD, an NIH user facility in the University of Illinois at Urbana-Champaign. It was constructed from a modified two-photon lifetime resolved microscope[59]. A schematic of the instrument's design is presented in Fig. 2.

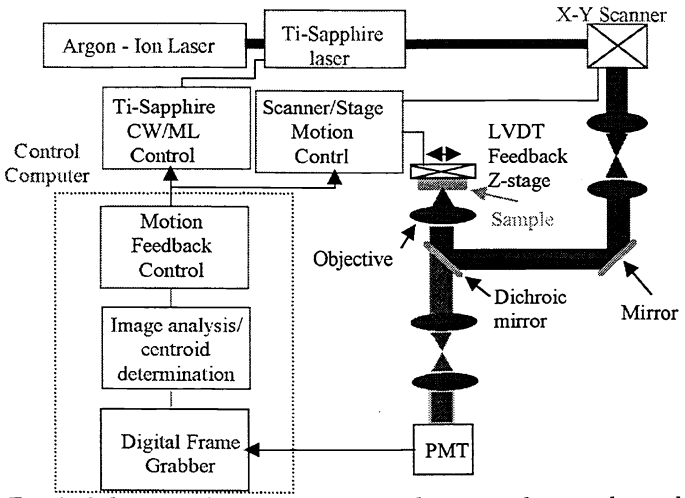

Fig. 2: Schematic diagram of the two-photon single particle tracking microscope

A critical element of this design is a mode-locked (ML) Titanium-Sapphire (Ti-Sapphire) laser (Mira 900) pumped by an Argon-Ion laser (Innova 310, Coherent Inc., Palo Alto, CA). This laser features a high average power of up to 1 W, a high pulse repetition rate of 80 MHz, and a short pulse width of 150 fs. High peak power is critical for efficient two-photon excitation. The beam expanded laser light is directed into the microscope via a galvanometer-driven x-y scanner (Cambridge Technology, Watertown, MA). The scanner accepts both digital and analog control signals and it feature random accessing of the scanner position. The nominal bandwidth of the scanner is 500 Hz. The excitation light enters the Zeiss Axiovert 35 microscope (Zeiss Inc., Thronwood, NY) via a modified epi-luminesence light path. Custom made dichroic mirrors (Chroma Technology Inc., Brattleboro, VT) reflects the collimated excitation to the objective. The objectives used in most of these

studies are Zeiss 63X Plan-Neofluar with numerical aperture of 1.25 and 40X Fluar with numerical aperture of 1.3. The z-axis position of the sample stage is controlled via a home built piezo-driven stage with a bandwidth of 50 Hz and a translation range of 6 μm. The fluorescence emission is collected by the objective and transmitted through the dichroic mirror along the emission path. An additional barrier filter consisting of 2 mm of BW39 bandpass filter (CVI Laser) eliminate most of the residual scatter with a minimum attenuation of the fluorescence signal in the blue-green region. A de-scan lens is inserted between the tube lens and the PMT. The de-scan lens re-collimates the fluorescence emission. It also ensures that the emission light strikes the PMT at a single position independent of scanner motion. The fluorescence signal at each pixel is detected by a photomultiplier tube (PMT). We use a low dark count R5600-P PMT (Hamamatsu, Bridgewater, NJ) with high quantum efficiency of 10% at 500 nm and 20% at 400 nm. A 100 MHz single photon counting discriminator (F-100T, Advanced Research Instruments, Boulder, CO) converts single photon bursts into TTL pulses. The number of collected photons are counted using a custom built interface circuit and transferred to the acquisition computer.

An essential element in this tracking system is the computer algorithm that coordinates image acquisition, particle position determination, and scanner/piezo-stage repositioning. In the vicinity of the particle, a series of three to five snapshots spanning an axial distance of about 2 microns are taken. The number of photons counted at each voxel is reconstructed into a three-dimensional image. The position of the particle is identified by locating the voxel of maximum intensity. The x-y scanner and the z stage are repositioned to center the particle in the volume. The snapshots and the scan origin are recorded in the computer RAM memory. A new series of snapshots is acquired at the new position and the feedback loop continues. A series of snapshots of a single latex particle diffusing in sucrose solution is presented in Fig. 3. Typical pixel residence time of these snapshots is 210 μs. A typical 10x10 pixel snapshot would require 20 ms which is the response bandwidth in the radial direction. Typically, three planes per volume, required to determine the axial position, corresponds to a bandwidth of 60 ms.

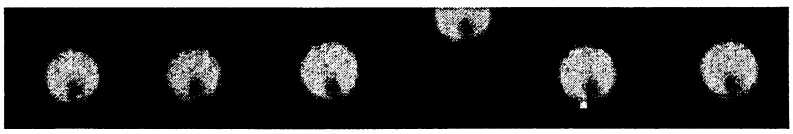

Fig. 3: A series of snapshots of a 2 μm latex sphere tracked by active feedback

A first generation optical trap particle delivery system was constructed. A very convenient approach is to use the same near infrared (NIR) beam from the Ti-Sapphire laser for both particle trapping and two-photon excitation. For particle trapping, about 200 mW of the Ti-Sapphire laser beam is conducted through the microscope excitation path. It is crucial that the Ti-Sapphire laser be operated in continuous wave (CW) mode; otherwise the fluorescent particles will be destroyed from over-heating due to excessive two-photon absorption. There is an added bonus of using the same laser beam for particle manipulation and tracking; it is possible to switch between trapping and tracking operations in a seamless fashion. Using a high power CW NIR beam, the particle can be positioned near the active site. By quickly dropping the IR power, switching the laser to a mode-locked operation, and engaging the feed-back control algorithm, we can commence tracking instantly.

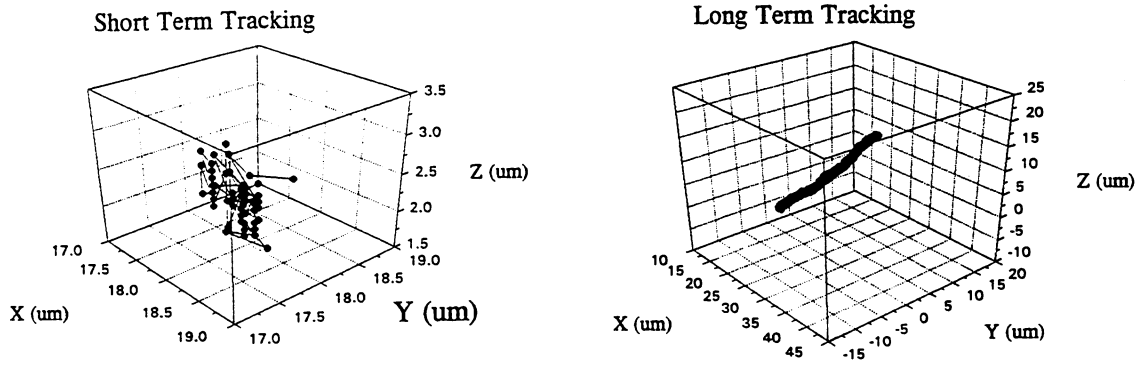

Fig. 4: The trajectory of a 0.47 μm latex sphere. Within any short period of time, the motion of the particle appears to be Brownian (upper figure). Over a longer period of time, the sphere's motion is directed by thermal convective current (lower figure).

5.2. Instrument calibration and characterization

To calibrate and characterize the prototype tracking system, we have followed the trajectory of individual latex spheres in sucrose solutions at various concentration. A representative trajectory of the diffusion of a 0.47 μm sphere is presented in Fig. 4. On a short time scale (about 1.5 seconds), the particle is observed to exhibit the expected isotropic Brownian trajectory. On a longer time scale (about 1 minute), we typically observe the particle motion is directed by thermal convection. Since particle tracking is intended to distinguish between directed and random Brownian motion, it is critical that the tracking system functions well even in the presence of directed motion with speed in excess of typical diffusion. From our data, a particle carried at a speed over 10 μm per second can be easily tracked.

The track of a drifting particle contains further information on the diffusion coefficient of the particle in the solvent. For a given drift velocity, a particle with larger diffusion coefficient will generate a wider track than that of a slower diffusing particle. Under the condition of slowly varying drift, it can be shown that diffusion coefficient, D, of a particle is related to the track length, L, the track width, W, and the tracking time, T (Fig. 5):

$$D \propto \frac{WL}{T} \tag{2}$$

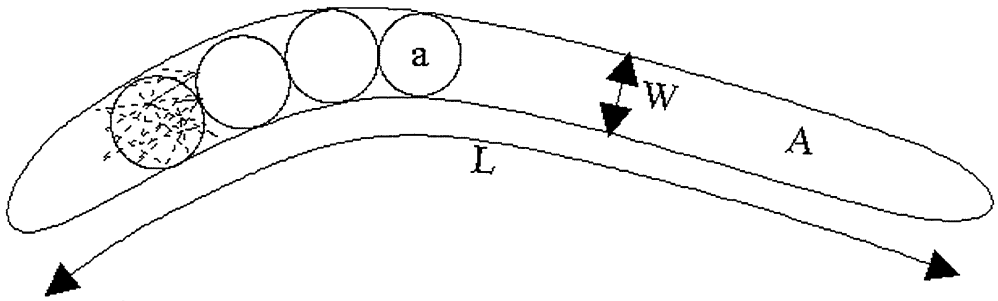

Fig. 5: A determination of the particle diffusion coefficient from its trajectory. For a short period of time t, a diffusing particle with diffusion coefficient D will cover a small circular area, a, where $a=2\pi Dt$. In the presence of a slow current, the particle will sweep out an area with a constant width, W and a length, L and in a time T. The total area A is equal to WL. This total area can be considered as a sum of the small circular areas. The number of these small area in the total area is just T/t. Therefore, $A=Ta/t=2\pi DT=WL$. The diffusion coefficient can be deduce to be: $D \propto WL/T$.

We have verified the precision of this instrument by measuring the diffusion of these latex spheres in solution. Spheres with 0.47 μm diameter were tracked in 18% (1.8 cp), 36% (4.6 cp) and 54% (25 cp) sucrose solutions. From the tracks measured at each concentration, we have calculated the diffusion coefficients of the spheres in these solutions. According to the Stoke Einstein equation, the diffusion coefficient is expected to vary inversely with the radius of the diffusers, and this was observed (Fig. 6).

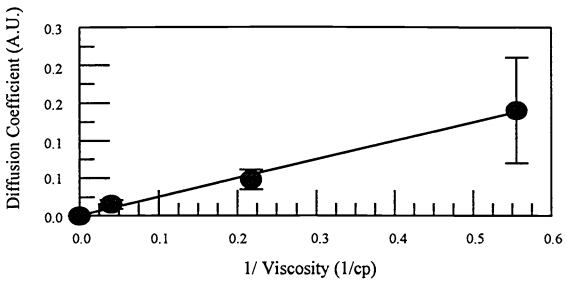

Fig. 6: The diffusion coefficient of 0.47 μm latex spheres as a function of sucrose solution viscosity

6. MACROPHAGE PHAGOCYTOSIS KINETICS

Phagocytosis is involved in many biological processes such as host immunological defense, tissue morphogenesis and intracellular infection by bacteria[66-69]. The understanding of phagocytosis is also crucial in the design of joint replacement implant[70]. Inflammatory reaction triggered by phagocytosis of wear debris by host macrophages is the major cause of loosening and osteolysis of total joint replacement. One major class of wear debris is sub-micron size polyethylene particles. By understanding the kinetics of polymeric particle phagocytosis and the subsequent release of cytokines, pharmacological interventions may be applied to prolong the lifetime of the implants. The study of macrophage phagocytosis of polymeric debris is an important biomedical problem for this 3-D SPT pilot study.

In this first study, we focused on the capture of antigenic material by murine fibroblast cells. In the presence of fluorescence latex spheres, rapid phagocytosis of this particles by these macrophages are readily observed (Fig. 7).

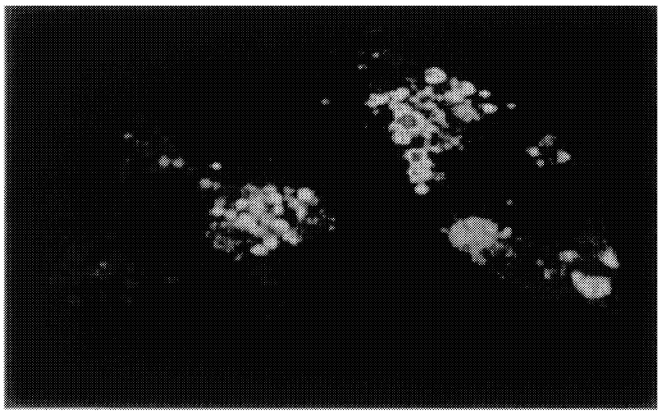

Fig. 7. Fluorescent vacuoles of macrophages are clearly visible after the phagocytosis of 0.4 μm latex spheres.

Murine fibroblast cells were grown on microscope cover slips until a density of about 100 cells per square millimeter was reached. The cover slip was mounted on a Teflon sample container and covered with 2 ml of growth medium. The container was mounted on the piezo-driven z-stage. For this first study, the cells were kept at room temperature. 1 μl solution (2% by volume) of 2.08 μm latex spheres was gently inserted into the bottom of a far corner in the container. Most of these spheres settled into a small region and formed a temporary repository of spheres. In the course of the experiment (about half an hour), a negligible number of spheres diffused to the vicinity of the cells of interest.

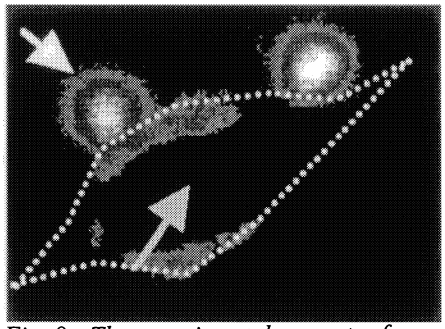

Fig. 8: The experimental geometry for macrophage capture of latex spheres. The center arrow indicates the position where the latex sphere was drop. The side arrow indicates the final position of the sphere. The fluorescent plasma membrane of the macrophage has been labeled with Laurdan after the sphere capture experiment. The brightly fluorescent round objects are the captured 2 μm latex spheres.

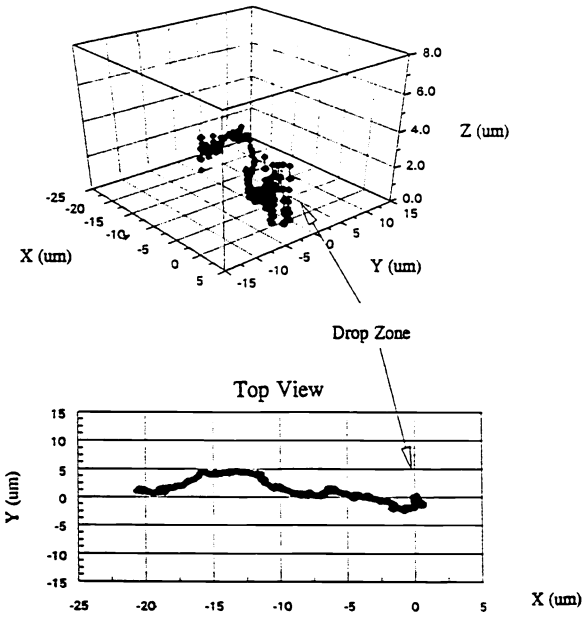

Fig. 9: The trajectory of a captured sphere. The top panel is the 3-D view and the bottom panel is the top view. Each time point in the trajectory is separated by 190 ms

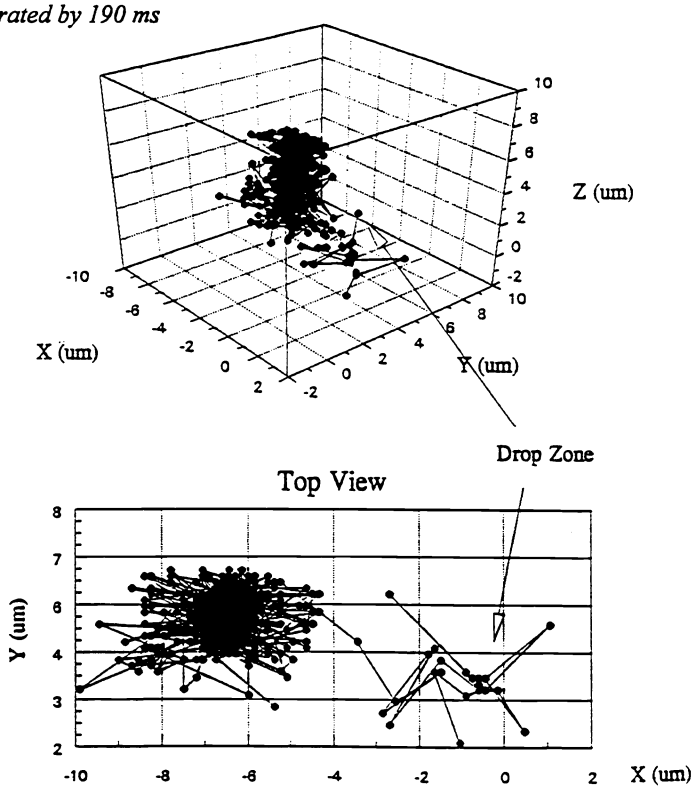

Fig. 10: The trajectory of a captured sphere. The top panel is the 3-D view and the bottom panel is the top view. Each time point in the trajectory is separated by 190 ms

Using the optical gradient trap system, we were able to capture and transport spheres to a chosen macrophage cell. The spheres were positioned about 2 to 5 μm above the center of the cell. With the tracking circuit ready, the spheres were released and tracking began. Since the lateral dimension of the cell is large, on the order of 100 square microns, the possibility that diffusion would bring the sphere placed in its proximity to the cell surface is high. While most of the spheres drifted away, we have observed active capture of some spheres by the cell. A typical release and capture geometry of the spheres by the macrophage cell is shown in Fig. 8. The track for the spheres that experienced some interaction but escaped is shown in Fig. 9. The trajectory of a captured sphere is unmistakable (Fig. 10). After initial release of the sphere, some Brownian diffusion was observed. At a short time later, a rapid lateral translation is observed corresponding to a movement of 5μm in less than 200 ms. Subsequent to the translation, the sphere is immobilized in the x-y plane within a diameter of 2 μm and within a axial position of 3 μm for the remainder of the experiment. After tracking, the sphere appears to be immobilized on the cell surface by visual inspection and the subsequent two-photon imaging generates Fig. 8. This observation suggests that we have observed the kinetics of active capture of an antigenic material by a macrophage cell and that the capture speed is over 25 μm/s. This the first 3-D particle tracking study of this important immunological system and we expect to perform more in-depth studies to confirm these results and to further follow the endocytosis process accompanied by spectroscopic measurements.

7. ACKNOWLEDGMENT

This work is supported by NIH grant R03155.

8. REFERENCES

1. A. Schwartz, "Cell biology of intracellular protein trafficking", Annu. Rev. Immunol. 8, 195-229, 1990.
2. B. V.Deures, O. W. Petersen, S. Olsnes, and K. Sandvig, Int. Rev. of Cytology, 117, 131-177, 1989.
3. C. Watts and M. Marsh, "Endocytosis: what goes in and how?" Journal of Cell Sciences, 103, 1-8, 1992.
4. I. Salmeen, P. Zacmanidis, G. Jesion and L. A. Feldkamp, "Motion of mitochondria in cultured cells quantified by analysis of digitized images", Biophys. J., 48, 681-686, 1985.
5. M. Socolovsky, A. R. Hockaday, J. M. Allen, "Human high-affinity Fc IgG receptor (FcγRI)-mediated phagocytosis nd pinocytosis in COS cells", Eur. J. of Cell. Biol., 64, 29-44, 1994.
6. S. Zimmerli, M. Majeed, M. Gustavsson, O. Stendahl, D. A. Sanan, and J. D. Ernst, "Phagosome-lysosome fusion is a calcium-independent event in macrophages", J. Cell. Biol., 132, 49-61, 1996.
7. R. C. Arduino, K. J. Palaz, B. E. Murray, and R. M. Rakita, "Resistance of Enterococcus faecium to neutrophil-mediated phagocytosis", Infection and Immunity, 62, 5587-5594, 1994.
8. C. J. Cohen, R. Bacon, M. Clarke, K. Joiner, and I. Mellman, "Dictyostelium discoideum mutants with conditional defects in phagocytosis", J. Cell Biol., 126, 955-966, 1994.
9. M. Maniak, R. Rauchenberger, R. Albrecht, J. Murphy, and G. Gerisch, "Coronin involved phagocytosis: dynamics of particle-induced relocalization visualized by a green fluorescent protein tag", Cell, 83, 915-924, 1995.
10. C. Dingwall, and R. Laskey, "The Nuclear Membrane", Science, 258, 942-947, 1992.
11. B. L. King, S. Vajda, C. Delisi, "Empirical free energy as a target function in docking and design—application to HIV-1 protease inhibitors", FEBS-LETTERS, 384, 87-91,.1996.
12. P. Gallay, V, Stitt, C., Mundy, M. Oettinger, D. Trono, "Role of karyoperin pathway in human immunodeficiency virus type 1 nuclear import", J. Virology, 70, 1027-1032, 1996.
13. R. E. Oneill, R. Jaskunas, G. Blobel, P. Palese, J. Moroianu, "Nuclear import of influenze virus RNA can be mediated by viral nucleoprotein and trasport factors required for protein import," J. Biol. Chem., 270, 22701-22704, 1995.
14. M. Marsh and A. Helenius, "Adsorptive endocytosis of Semliki Forest virus", J. Mol. Biol., 142, 439-454, 1980.
15. K. Sandvig, O. Gerred, K. Prydz, J. V. Kolov, S. H. Hansen, and b. V. Deurs, "Retrograde transport of endocytosed Shiga toxin to the endoplasmic reticulum", Nature, 358, 510-512, 1992.
16. C. Montecucco, E. Papini, G. Schiavo, "Bacterial protein toxin penetrate cells via a four step mechanism", FEBS Let, 346, 92-98, 1994.
17. Y. K. Oh and R. M. Straubinger, "Intracellular Fate of Mycobacterium avium: Use of dual-label spectrofluorometry to investigate the influence of bacterial viability and opsonization on phagosomal pH and phagosome-lysosome interaction", Infection and Immunity, 64, 319-325, 1996.

18. M. Watarai, S. Funato, and C. Sasakawa, "Interaction of Ipa proteins of Shigella Flexneri with $\alpha_5\beta_1$ Integrin promotes entry of baceria into mammalian cells", J. Exp. Med. 183, 991-999, 1996.

19. J. H. Morisaki, J. E. Heuser, and L. D. Sibbley, "Invasion of Toxoplasma gondii occur by active penetration of the host cell", J. Cell. Sci., 108, 2457-2464, 1995.

20. M. J. Brickman, J. M. Cook, and A. E. Balber, "Low temperature reversibly inhibits transport from tubular endosomes to a pernuclear, acidic compartment in African trypanosomes", J. Cell Sci., 108, 3611-3621, 1995.

21. J. Adovelande, Y. boulard, J. P. Berry, P. Galle, G. Slodzian, and J. Schrevel, "Detection and cartography of the fluorinated antimalarial drg mefoquine in normal and plasmodium falciparum inflected red cells by scanning ion microscopy and mass spectroscopy", Biol. Cell., 80, 185-192, 1994.

22. M. D. Miliotis, B. D. Tall, and R. T. Gray, "Adherence to and invasion of tissue culture cells by vibrio hollisae", Infection and immunity, 63, 4959-4963, 1995.

23. J. E. Rothman, "Mechanism of intracellular protein transport", Nature, 372, 55-63, 1994.

24. J. L. Goldstein, M. S. Brown, R. G. W. Anderson, D. W. Russell, and W. J. Schneider, "Receptor-mediated endocytosis: concepts emerging from the LDL receptor system", Ann Rev Cell Biol., 1, 1-39, 1985.

25. D. Moss, A. R. Hibbs, D. Stenzel, L. W. Powell and J. W. Halliday, "The endocytic pathway for H-ferritin established in live MOLT-4 cells by laser scanning confocal microscopy", Brit. J. Haematology, 88, 746-753, 1994.

26. A. L. Schwartz, S. E. Fridovich and H. F. Lodish, "Kinetics of internalization and recycling of the Asiaoglycoprotein receptor in hepatoma cell line", J. Biol. Chem., 257, 4230-4237, 1982.

27. P. H. Weigel and J. A. Oka, "Endocytosis and degradation mediated by the Asialoglcoprotein receptor in isolated rat hepatocytes", J. Biol.Chem., 257, 1201-1207, 1982.

28. T. Barzu, M. Pascal, M. Maman, C. Roque, F. Lafont, and A. Rousselet, "Entry and distribution of fluorescent antiproliferative heparin derivatives into rat vascular smooth muscle cells: comparison between heparin-sensitive and heparn-resistant cultures", J. Cell. Physiology, 167, 8-21, 1996.

29. R. N. Ghosh and W. W. Webb, "Results of automated tracking of low density lipoprotein receptors on cell surfaces", Biophys. J., 53: 352a, 1988.

30. R. N. Ghosh and W. W. Webb, "Automated detection and tracking of individual and clustered cell surface low density lipoprotein receptor molecules", Biophys. J., 66, 1301-1318, 1994.

31. D. Axelrod, D. E. Koppel, J. Schlessinger, E. Elson and W. W. Webb, "Mobility measurement by analysis of fluorescence photobleaching recovery kinetics", Biophys J., 16, 1055-1069, 1976.

32. J. Gelles, B. J., Schnapp, M. P. Sheetz, "Tracking of kinesin-driven movements with nanometer-scale precision", Nature, 331, 450-453, 1988.

33. M. J. Saxton, "Single-particle tracking: models of directed transport", Biophys. J., 67, 2110-2119, 1994.

34. K. Jacobson, E. D.. Sheets, and R. Simson, "Revisiting the fluid mosaic model of membranes", Science, 268, 1441-1442, 1995.

35. C. E. Schmidt, T. Chen, and D. A. Lauffenburger, "Simulation of Integrin-Cytoskeletal interaction in migrating fibroblasts", Biophys. J., 67, 461-474, 1994.

36. C. E. Schmidt, A. F. Horwitz, D. A. Lauffenburger, and M. P. Sheetz, "Integrin-cytoskeletal interactions in migrating fibroblasts are dynamic, asymmetric and regulated", J. Cell Biol, 123, 977-991, 1993.

37. M. P. Sheetz, S. Turney, H. Qian, and E. L. Elson, "Nanometer-level analysis demonstrates that lipid flow does not drive membrane glycoprotein movement", Nature(Lond.), 340, 284-288, 1989.

38. B. W. Hicks and K. J. Angelides, "Trackig movement of lipids and Thy 1 molecules in the plasmalemma of living fibroblasts by fluorescence video microscopy with nanometer scale precision", J. Mem. Biol., 144, 231-244, 1995.

39. Y. L. Wang, J. D. Silverman, and L. G. Cao, "Single particle tracking of surface receptor movement during cell division", J. Cell Biol., 127, 963-971, 1994.

40. M. Fein, J. Unkeless, F. Y. S. Chuang, M. Sassaroli, R. D. Costa, H. Vaananen, J. Eisinger, "Lateral mobility of lipid analogues and GPI-anchored proteins in supported bilayers determined by fluorescent bead tracking", J. Mem. Biol., 133, 83-92, 1993.

41. H. P. Kao and A. S. Verkman, "Tracking of single fluorescent particles in three dimensions: use of cylindrical optics to encode particle position", Biophys. J., 67, 1291-1300, 1994.

42. W. Denk, W., J. H. Strickler and W. W. Webb, "Two-photon laser scanning fluorescence microscopy", Science, 248, 73-76, 1990.

43. R. R. Birge, "One-photon and two-photon excitation spectroscopy," *Ultrasensitive laser spectroscopy,* Kliger, ed., 109-174, Academic Press, New York, 1983.

44. R. R. Birge, "Two-photon spectroscopy of protein-bound chromophores", Acc. Chem. Res., 19, 138-146, 1985.
45. S. M. Kennedy and F. E. Lytle, "p-Bis(o-methylstyryl)benzene as a power squared sensor for two-photon absorption measurements between 537 and 694 nm", Anal. Chem., 58, 2643-2647, 1986.
46. S. Jiang, "Two-photon spectroscopy of biomolecules", Prog. React. Kinet., 15, 77-92, 1989.
47. T. Wilson, and C. Sheppard, *Theory and practice of scanning optical microscopy,* Academic Press, New York, 1984.
48. C. J. R. Sheppard and M. Gu, "Image formation in two-photon fluorescence microscopy", Optik, 86, 104-6, 1990.
49. O. Nakamura, "Three-dimensional imaging characteristics of laser scan fluorescence microscopy: two-photon excitation vs single-photon excitation", Optik, 93, 39-42, 1992.
50. A. Ashkin, "Trapping of atoms by resonance radiation pressure", Phys. Rev. Lett., 40, 729-732, 1978.
51. K. Svoboda and S. M. Block, "Biological applications of optical forces", Annu. Rev. Biophys. Biomol. Struct. 23, 247-285, 1994.
52. R. Y. Tsien and A. Waggoner, "Fluorophores for confocal microscopy" *Handbook of biological confocal microscopy*, J. Pawley, ed., 267-281, Plenum Press, New York, 1995.
53. C. Xu and W. W. Webb, "Measurement of two-photon excitation cross section of molecular fluorophores with data from 690 to 1050 nm", J. Opt. Soc. Am. B, 13, 481-491, 1996.
54. W. M.Yu, P. T. C. So, T. French, and E. Gratton, "Fluorescence Polarization of Cell Membrane -- A Two-Photon Scanning Microscopy Approach", Biophys. J., 70, 626-636, 1996.
55. R. Y. Tsien and A. T. Harootunian, "Practical design criterion for a dynamic ratio imaging system", Cell Calcium, 11, 93-109, 1990.
56. R. M. Clegg, "Fluorescence Resonance Energy Transfer", *Fluorescence Imaging Spectroscopy and Microscopy,* Wang and Herman ed., 179-253, Wiley & Sons, New York, 1996.
57. S. M. Blackman, C. E. Cobb, A. H. Beth, and D. W. Piston, "The orientation of eosin 5 maleimide on human erythrocyte band 3 measured by fluorescence polarization microscopy", Biophys. J., 71, 194-208, 1996.
58. D. Axelrod, "Carbocyanine dye orientation in red cell membrane studied by microscopic fluorescence polarization", Biophys. J., 26, 557-573, 1979.
59. P. T. C. So, T. French, W. M. Yu, K. M. Berland, C. Y. Dong, and E. Gratton, "Time-resolved fluorescence microscopy using two-photon excitation", Bioimaging, 3, 49-63, 1995.
60. T. W. J. Gadella, Jr., T. M. Jovin and R. M. Clegg, "Fluorescence lifetime imaging microsocpy (FILM): Spatial resolution of microstructures on the nanosecond time scale", Biophys. Chem., 48, 221-39, 1993.
61. C. G. Morgan, A. C. Mitchell, and J. G. Murray, "Prospects for confocal imaging based on nanosecond fluorescence decay time", J. Microsc., 165, 49-60, 1991.
62. T. Oida, Y. Sako, and A. Kusumi, "Fluorescence lifetime imaging microscopy (filmscopy)", Biophys. J., 64, 676-685, 1993.
63. E. P. Buurman, R. Sanders, A. Draaijer, H. C. Gerritsen, J. J. F. van Veen, P. M. Houpt, and Y. K. Levin, "Fluorescence lifetime imaging using a confocal laser scanning microscope", Scanning, 14, 155-9, 1992.
64. M. Eberhard, and P. Erne, "Calcium binding to fluorescent calcium indicators: calcium green, calcium orange, and calcium crimson", Biochem, Biophys. Res. Comm., 180, 209-15, 1991.
65. J. R. Lakowicz, H. Szmacinski, and M. L. Johnson, "Calcium imaging using fluorescence lifetime and long wavelength probes", J. Fluoresc., 2, 47-62, 1992.
66. M. Socolovsky, A. R. Hockaday, J. M. Allen, "Human high-affinity Fc IgG receptor (FcγRI)-mediated phagocytosis nd pinocytosis in COS cells", Eur. J. of Cell. Biol., 64, 29-44, 1994.
67. S. Zimmerli, M. Majeed, M. Gustavsson, O. Stendahl, D. A. Sanan, and J. D. Ernst, "Phagosome-lysosome fusion is a calcium-independent event in macrophages", 132, 49-61, 1996.
68. R. C. Arduino, K. J. Palaz, B. E. Murray, and R. M. Rakita, "Resistance of Enterococcus faecium to neutrophil-mediated phagocytosis", Infection and Immunity, 62, 5587-5594, 1994.
69. B. Tycko and F. R. Maxfield, "Rapid acidification of endocytic vesicles containing α_2-Macroglobulin", Cell, 28, 643-651, 1982.
70. T. M. Wright and S. B. Goodman, ed., *Implant Wear: The Future of Total Joint Replacement*, American Academy of Orthopaedic Surgeons, 1996.